



The dorsomedial prefrontal cortex prioritizes social learning during rest

Courtney A. Jimenez^a and Meghan L. Meyer^{a,1}

Edited by Emily B. Falk, University of Pennsylvania, Philadelphia, PA; received June 1, 2023; accepted February 12, 2024 by Editorial Board Member Michael S. Gazzaniga

Sociality is a defining feature of the human experience: We rely on others to ensure survival and cooperate in complex social networks to thrive. Are there brain mechanisms that help ensure we quickly learn about our social world to optimally navigate it? We tested whether portions of the brain's default network engage “by default” to quickly prioritize social learning during the memory consolidation process. To test this possibility, participants underwent functional MRI (fMRI) while viewing scenes from the documentary film, *Samsara*. This film shows footage of real people and places from around the world. We normed the footage to select scenes that differed along the dimension of sociality, while matched on valence, arousal, interestingness, and familiarity. During fMRI, participants watched the “social” and “nonsocial” scenes, completed a rest scan, and a surprise recognition memory test. Participants showed superior social (vs. nonsocial) memory performance, and the social memory advantage was associated with neural pattern reinstatement during rest in the dorsomedial prefrontal cortex (DMPFC), a key node of the default network. Moreover, it was during early rest that DMPFC social pattern reinstatement was greatest and predicted subsequent social memory performance most strongly, consistent with the “prioritization” account. Results simultaneously update 1) theories of memory consolidation, which have not addressed how social information may be prioritized in the learning process, and 2) understanding of default network function, which remains to be fully characterized. More broadly, the results underscore the inherent human drive to understand our vastly social world.

social cognition | default network | memory | DMPFC | fMRI

As we move through everyday life, we come across an abundance of information. Just as an example, imagine walking through your favorite city. At once, you are bombarded with signs, shops, and people interacting in all kinds of ways. We continuously perceive far more than we could possibly remember (1–3). Some experiences stick with us, and others are forgotten (4). Is certain information from our seemingly seamless encoding prioritized in memory, and if so, how?

One possibility is that social information may be prioritized in memory. Consistent with prior social psychology research, here “social information” refers to data about agents conveying a mind and the thoughts and feelings we need to infer to comprehend it (5–7). Given that primates rely on conspecifics to ensure survival (8–11), social information is highly valuable (12), which should amplify its memorability (13–15). There is also evidence that social content tends to be easily learned and retrieved (16, 17). For instance, the same stimulus is more memorable if participants attend to its social (vs. nonsocial) aspects during encoding (16, 18). Past social stressors (e.g., a romantic break-up) are also more easily reexperienced than past nonsocial stressors (e.g., a physical injury), even when the events are matched on emotional intensity at the time of the event (19). Social information can even be used to potentiate reinforcement learning as early in development as infancy (17). Collectively, psychological data point to the possibility that social information carries a powerful memorial glue.

If social information is privileged in memory, how might the brain prioritize it during the learning process? An answer to this question may stem from two observations. First, the brain region most reliably associated with social information processing, the dorsomedial prefrontal cortex (DMPFC; 20–23), is also part of the brain's default network, known to engage quickly by default during rest (24–26). More specifically, the default network shows strong, endogenous engagement during rest. In fact, this network shows greater activation during rest periods relative to many cognitive tasks, which is why it has been termed the “default network” or “default mode network” (24–26). Second, rest is a time when new information is committed to memory (i.e., consolidated; 27–29). The tendency for the human brain to “default” (i.e., show strong endogenous activation) to

Significance

Writer Kurt Vonnegut once said “if you describe a landscape or a seascape, or a cityscape, always be sure to include a human figure somewhere in the scene. Why? Because readers are human beings, mostly interested in other human beings.” Consistent with Vonnegut's intuition, we found that the human brain prioritizes learning scenes including people, more so than scenes without people. Specifically, as soon as participants rested after viewing scenes with and without people, the dorsomedial prefrontal cortex of the brain's default network immediately repeated the scenes with people during rest to promote social memory. The results add insight into the human bias to process the social landscape.

Author affiliations: ^aDepartment of Psychology, Columbia University, New York, NY 10027

Author contributions: C.A.J. and M.L.M. designed research; C.A.J. performed research; C.A.J. analyzed data; and C.A.J. and M.L.M. wrote the paper.

The authors declare no competing interest.

This article is a PNAS Direct Submission. E.B.F. is a guest editor invited by the Editorial Board.

Copyright © 2024 the Author(s). Published by PNAS. This open access article is distributed under [Creative Commons Attribution-NonCommercial-NoDerivatives License 4.0 \(CC BY-NC-ND\)](https://creativecommons.org/licenses/by-nc-nd/4.0/).

¹To whom correspondence may be addressed. Email: meghan.meyer@columbia.edu.

This article contains supporting information online at <https://www.pnas.org/lookup/suppl/doi:10.1073/pnas.2309232121/-/DCSupplemental>.

Published March 11, 2024.

the DMPFC as soon as our mind is free of external demands may therefore bias us toward social memory consolidation during rest.

Although memory consolidation often operates on long timescales (30)—for example, over a night of sleep (31, 32)—prior work has shown that neural responses directly after encoding make important contributions to the memory consolidation process (33, 34). On the topic of memory “prioritization,” prior work shows that some stimuli may be prioritized over others in the consolidation process that occurs directly following encoding (35). On the topic of social information processing, prior research indicates that higher spontaneous DMPFC activity before a stimulus predicts faster subsequent social information processing for the immediately following stimulus (36, 37). In other words, when endogenous DMPFC activity is strong during brief rest, it accelerates social cognition. Here, we examined whether endogenous DMPFC processes directly after encoding social information prioritize its consolidation, perhaps by also helping it happen relatively quickly.

Consistent with this possibility, past work implicates the DMPFC in social memory encoding and retrieval (18, 23, 38), and the DMPFC may play a general role in social learning during rest (39, 40). For example, the DMPFC increases functional connectivity with other portions of the default network after encoding new social information, and this increased connectivity predicts social (but not nonsocial) subsequent memory performance (39, 40). Critically, however, past work examining social consolidation during rest fully separates social encoding from nonsocial encoding to isolate which brain regions consolidate the different information during rest. As a result, it is impossible to know whether social consolidation is “prioritized” at rest by the DMPFC based on prior research; a claim for prioritization would require evidence that when presented with social and nonsocial information during the same encoding session, the DMPFC prefers to consolidate the social information during subsequent rest and possibly does so more quickly than brain regions outside of the default network consolidating other forms of information. Establishing the prioritization of social consolidation would update existing theories of learning and memory, which to date have not considered this possibility. This gap is surprising, given that theoretical accounts of memory formation suggest that goal-relevant content may be prioritized during consolidation (41) and that humans have a strong, endogenous goal to feel connected to their social world (42).

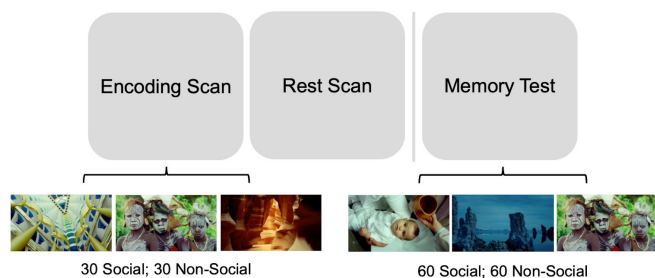
The hypothesis driving the present study is that social information is prioritized during consolidation at rest in the DMPFC. Strong evidence for this possibility requires anticipating and thwarting two potential confounds. First, social information is

often conflated with a number of dimensions known to enhance memory: valence, arousal, interestingness, and familiarity (43–45). If we found that the DMPFC consolidated social memory during early rest, it would be hard to know whether it is the “socialness” of the information encoded (i.e., the extent to which it pertained to people) that drove prioritization vs. the other dimensions with which socialness tends to covary. Second, to best approximate real-world social learning, it is important to use encoding stimuli that are as naturalistic as possible, yet a great deal of naturalistic social stimuli used in neuroscience research take the form of a narrative story (46). Many naturalistic approaches to investigating the role of the default network in social cognition involve television dramas, movies, and podcasts (47–51). However, the narrative plot of these stories creates a confound for the present hypotheses. For example, imagine participants encoded a story while undergoing fMRI (functional MRI), and it was found that they had better memory for the social (vs. nonsocial) information in the story and that the DMPFC prioritized social consolidation at rest. In this scenario, it would be difficult to determine whether the social memory advantage was due to the prioritization of social learning at rest broadly speaking or whether the plot of the story creates an organizational structure for social information (but not nonsocial information), which could incidentally improve and prioritize social memory.

To rule out these confounds, we presented participants with footage from the documentary film, *Samsara*. This documentary was intentionally developed to have no narrative or plot and instead portrays footage of real people, places, and objects from around the world. Scenes from the documentary were normed by independent raters on valence, arousal, interestingness, familiarity, and socialness. This allowed us to select a subset of video clips that varied on the dimension of sociality, while being matched on the other dimensions. With this paradigm in hand, we next had a new sample of participants complete fMRI while they encoded the social and nonsocial video clips in a fully intermixed fashion, completed a rest scan, and a surprise memory test for the footage (Fig. 1A).

If the social prioritization account is correct, we would expect to see the following patterns in our data. First, participants should show better memory performance for the social vs. nonsocial stimuli. Second, we should see evidence that the DMPFC preferentially consolidates the social information encoded (but not nonsocial information encoded), and this consolidation may occur during early stages of rest. This would be consistent with the idea that our tendency to default to the DMPFC as soon as we rest (i.e., show strong endogenous activation) biases the brain toward

A Paradigm



B Memory Performance

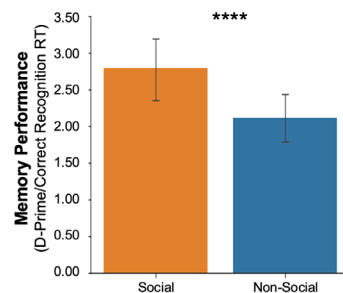


Fig. 1. (A) Experimental paradigm. Participants encode social and nonsocial video clips from *Samsara* in a randomized order and undergo a subsequent rest scan. Next, participants complete a surprise recognition memory test that includes all of the 60 videos encoded, as well as 60 lure videos that were not previously encoded. Social and nonsocial videos are matched on valence, arousal, interestingness, and familiarity and differ on the dimension of sociality: the extent to which they have to do with people. (B) Memory performance. Participants demonstrated better social vs. nonsocial memory performance. Error bars reflect 95% CIs.

social memory consolidation. We used a neural pattern reinstatement approach to test this hypothesis (33, 35). This approach tests whether reengaging multivariate patterns from encoding during subsequent rest predicts memory performance (35). The reinstatement approach is conceptually similar to the idea of “replay” during rest from the rodent literature on memory consolidation (52–55).

To complement our hypotheses about the DMPFC in social consolidation, we also investigated whether pattern reinstatement in a prefrontal brain region traditionally associated with nonsocial memory—the left ventrolateral prefrontal cortex (IVLPFC; 56)—may show evidence of neural pattern reinstatement during rest for the nonsocial (but not social) stimuli. Given that the IVLPFC is not a region that is more associated with rest relative to cognitive tasks, we predicted that the IVLPFC would show nonsocial reinstatement across the rest period generally, as opposed to prioritization during early rest in particular. Finally, given that the hippocampus is thought to play a general role in memory consolidation (27, 57), we also examined whether this brain region shows evidence of both social and nonsocial memory consolidation during rest.

Results

Better Memory Performance for Social (vs. Nonsocial) Videos.

Our first prediction is that participants will show better memory performance on the surprise memory test for the social (vs.

nonsocial) video clips from *Samsara*. The surprise memory test was structured such that participants were shown images from the 60 encoded (30 social; 30 nonsocial) and 60 lure video clips (30 social; 30 nonsocial) in a fully randomized order. The lure video clips were normed on valence, arousal, interestingness, and familiarity in the same fashion as the encoded stimuli (*Methods*). Consistent with our first prediction, participants showed superior social (vs. nonsocial) memory performance [$t(24) = 5.06, P = 3.612e-05$; Fig. 1*B*]. We define memory performance here as the d' memory score (by subtracting standardized false alarms from standardized hits with z-scores derived via the inverse cumulative density function) divided by the correct reaction time (RT) so that our memory performance score considers both accuracy and speed and because this variable showed more variability across participants than d' alone. It is noteworthy that social memory performance remains significantly better than nonsocial memory performance even if we only consider d' as our measure of accuracy [$t(24) = 5.09, P = 3.735e-05$] or just correct RT as our measure of accuracy [$t(24) = -2.87, P = 8.595e-03$]. Thus, the behavioral results robustly suggest social information is better recalled than nonsocial information, even when constructs often conflated with sociality (i.e., valence, arousal, interestingness, and familiarity) are held constant.

Double Dissociation for Social (DMPFC) and Nonsocial (IVLPFC) Consolidation Mechanisms during Rest. We created regions of interest (ROIs) of the DMPFC cluster observed in the contrast of

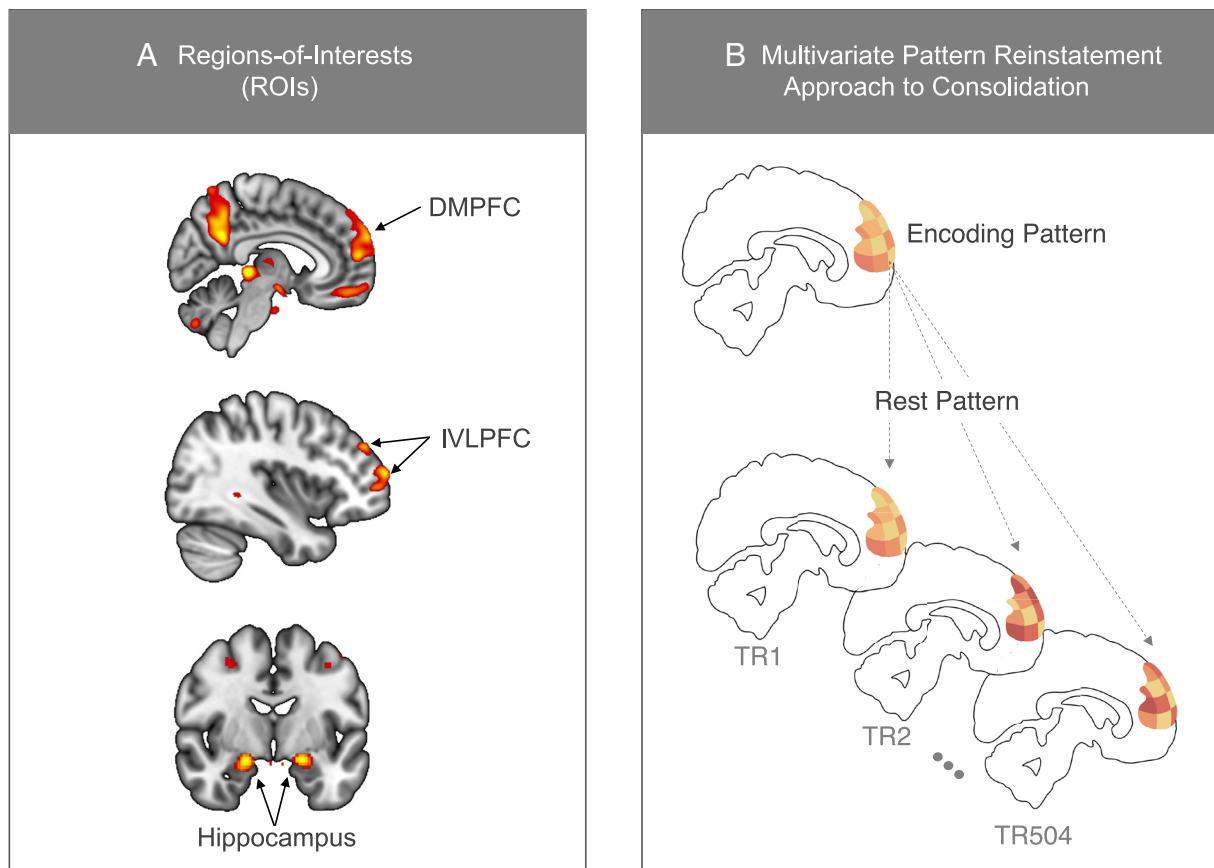


Fig. 2. (A) ROIs predicted to show reinstatement and subsequent memory effects. DMPFC refers to the dorsomedial prefrontal cortex, which was predicted to show social reinstatement and subsequent social memory effects. IVLPFC refers to the left ventrolateral prefrontal cortex and was predicted to show nonsocial reinstatement and subsequent nonsocial memory effects. The hippocampus, given its broad role in memory, was predicted to show reinstatement and subsequent memory effects collapsed across social and nonsocial content. (B) Visual depiction of the reinstatement approach in which the multivariate patterns in a ROI during encoding are applied to each TR of the subsequent rest scan. In line with prior work (35), correlations between the encoding pattern and TR rest pattern that are 1.5 SDs above the mean for a given subject are considered instances of reinstatement.

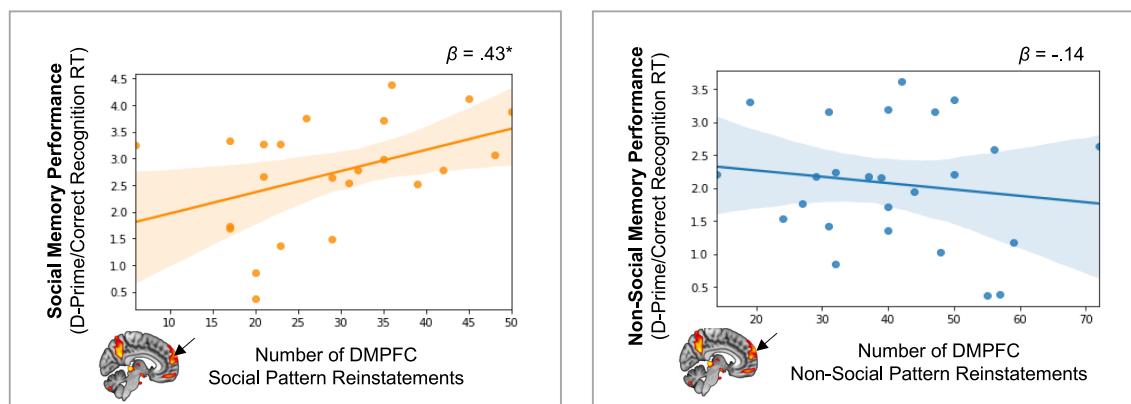
social (vs. nonsocial) encoding and the IVLPFC cluster observed in the contrast of nonsocial (vs. social) encoding (Fig. 2A; see *Methods* for information on ROIs). Each subject's multivariate pattern in the ROIs during social video encoding, and separately, nonsocial video encoding were extracted. Next, we performed the reinstatement analysis developed by Schapiro et al. (35; Fig. 2B). The approach, conceptually, is template matching: identifying instances during rest in which the multivariate DMPFC pattern is meaningfully similar to the pattern observed during encoding and linking the number of reinstatements to subsequent memory performance (see *Methods* for more details). The observed reinstatement events showed high correlations with encoding patterns (Means > 0.59; SDs < 0.064), which further supports and justifies counting these instances as reinstatement.

Consistent with the hypothesis that the DMPFC preferentially consolidates social information, the number of DMPFC social pattern reinstatements across the rest period predicted social memory performance ($\beta = 0.43$, $P = 0.042$; Fig. 3A), whereas the number of nonsocial pattern reinstatements in the DMPFC across the rest period was unrelated to nonsocial memory performance ($\beta = -0.14$, $P = 0.505$, Fig. 3A). Follow-up analyses directly comparing these two beta estimates showed they were significantly different from one another ($z = 2.07$, $P = 0.019$, one-tailed). The IVLPFC showed the opposite pattern of results. The number of IVLPFC nonsocial pattern reinstatements significantly predicted nonsocial memory performance ($\beta = 0.42$; $P = 0.040$; Fig. 3B), whereas the

number of IVLPFC social pattern reinstatements was unrelated to social memory performance ($\beta = -0.03$; $P = 0.880$; Fig. 3B). Follow-up analyses directly comparing these two beta estimates showed they were marginally different from one another ($z = 1.58$, $P = 0.057$, one-tailed). It is noteworthy that, overall, there was a greater number of nonsocial (vs. social) DMPFC pattern reinstatements [$t(23) = -2.45$, $P = 0.023$; mean social DMPFC = 29.00 SD = 10.85; mean nonsocial DMPFC = 39.96 SD = 12.01], although as noted above and shown in Fig. 3A, the number of nonsocial DMPFC pattern reinstatements do not significantly relate to nonsocial memory performance (whereas the number of DMPFC social pattern reinstatements do significantly relate to social memory performance).

As an additional check on the robustness of these relationships, we ran control analyses in which we generated an encoding template for which the beta values were randomly sampled from the social and nonsocial encoding templates. Thus, this template consisted of a mix of partial social and nonsocial representations at encoding randomly spatially distributed throughout the template. Mixed DMPFC pattern reinstatement did not meaningfully relate to social memory performance ($\beta = 0.03$, $P = 0.884$), nor did mixed IVLPFC pattern reinstatement relate to nonsocial memory performance ($\beta = 0.30$, $P = 0.138$). Further, we ran another control analysis in which the encoding template was simply the average of both the social and nonsocial encoding templates, thus representing all stimuli at encoding. Again, average DMPFC

A DMPFC Reinstatement – Memory Relationships



B IVLPFC Reinstatement – Memory Relationships

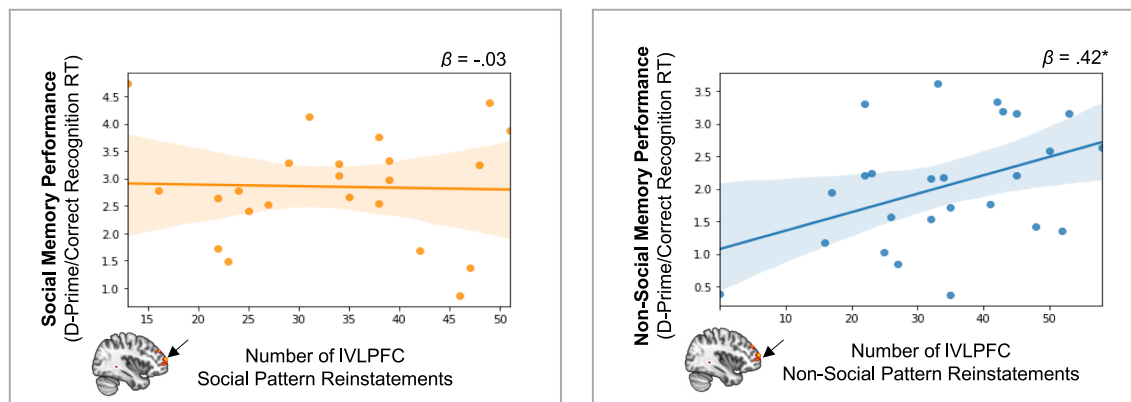


Fig. 3. Double dissociation for social and nonsocial memory consolidation. Panel (A) shows that DMPFC social pattern reinstatement significantly predicts social, but not nonsocial, memory performance. Panel (B) shows that IVLPFC nonsocial pattern reinstatement significantly predicts nonsocial, but not social, memory performance.

pattern reinstatement did not meaningfully relate to social memory ($\beta = 0.12$, $P = 0.592$), nor did average IVLPFC pattern reinstatement relate to nonsocial memory ($\beta = 0.16$, $P = 0.452$). These analyses further support the specificity of our results to the sociality of the given stimuli.

Although our hypotheses were specific to the DMPFC and IVLPFC, to ensure we did not miss any meaningful patterns in other brain regions, we ran two follow-up analyses. First, we assessed whether the relationship between the number of neural pattern reinstatements during rest and subsequent memory was significant in the other ROIs observed during encoding (social vs. nonsocial encoding: VMPFC; precuneus, left amygdala, and fusiform gyrus; nonsocial vs. social encoding: bilateral parahippocampal place area). None of these follow-up analyses were significant (β 's < 0.208, P 's > 0.318), except for the IPPA showing a significant (and negative) nonsocial reinstatement-to-subsequent nonsocial memory relationship ($\beta = -0.54$, $P = 0.007$). Second, given that it is possible regions outside of those observed during encoding could show evidence of reinstatement-to-subsequent memory effects, we next repeated our reinstatement analyses with a $k = 50$ whole-brain parcellation (58). No additional brain regions showed support for this possibility. Collectively, these results suggest that the link between greater neural pattern reinstatement during rest and superior subsequent memory is supported by different prefrontal regions for social (DMPFC) and nonsocial (IVLPFC) memory.

The DMPFC Shows Evidence of Social Consolidation during Early Stages of Rest.

Given that we established that DMPFC social pattern reinstatements relate to social (but not nonsocial) memory performance, while IVLPFC nonsocial pattern reinstatements relate to nonsocial (but not social) memory performance, we next sought to dig deeper into how the DMPFC may prioritize social learning during rest. The definition of "prioritize" is to treat something as more important than other things. Our next question was whether the brain prioritizes DMPFC social pattern reinstatement by doing it early in the consolidation process. That is, does social consolidation happen relatively quickly in the DMPFC? To examine this possibility, we simply divided our resting state scan into early (0 to 168 s), middle (168 to 336 s), and late (336 to 504 s) time periods and summed the number of DMPFC social pattern reinstatements in each time period. We then used a linear mixed effects model to test the within-subjects contrast that the number of reinstatements during the early portion of rest is significantly greater than the middle and late rest periods (i.e., $2/3_{\text{early}} - 1/3_{\text{middle}} - 1/3_{\text{late}}$), which was significant [$t(44) = 3.04$, $P = 0.004$; Fig. 4]. Moreover, the relationship between the number of DMPFC social pattern reinstatements and social memory performance is driven by early rest: When DMPFC social pattern reinstatement for early, middle, and late rest was entered as separate regressors in a model predicting social memory performance, only early rest significantly predicted social memory performance ($\beta = 0.61$, $P = 0.006$). Follow-up analyses further confirmed this effect, showing the relationship is significant during

the early rest period ($\beta = 0.58$, $P = 0.004$) but not the middle ($\beta = 0.12$, $P = 0.600$) or late rest periods ($\beta = 0.19$, $P = 0.391$, Fig. 5). See *SI Appendix* for a replication of these results at the item level, when only sustained reinstatement instances are counted, and when hits are used as the outcome variable.

The same analysis with the nonsocial DMPFC encoding template produced null results: The number of nonsocial pattern reinstatements in the DMPFC was not greater during early vs.

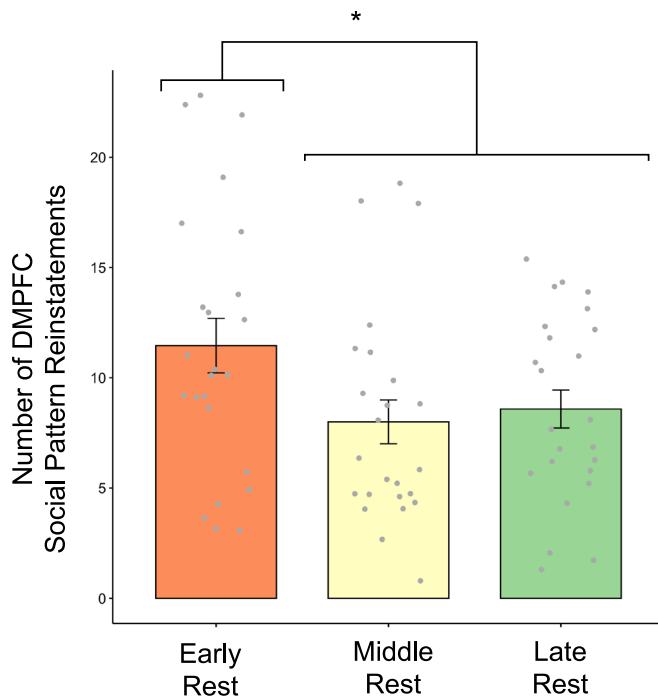


Fig. 4. The DMPFC shows a greater number of social pattern reinstatements during early (vs. middle and late) portions of the rest scan. Error bars reflect 95% CIs.

middle and late periods of rest [$t(44) = 1.46$, $P = 0.152$]. Additionally, the number of nonsocial pattern reinstatements in the DMPFC was unrelated to nonsocial memory performance during early, middle, and late rest periods (β 's < 0.259, P 's > 0.211).

We next ran a follow-up, exploratory analysis to further isolate when during early rest the DMPFC social pattern reinstatements meaningfully predict social memory performance. We performed a sliding window analysis in which we set the window of time to 36 TRs. We selected this amount of time so that the first snapshot of time was long enough to have a reliable estimate of reinstatement counts and an even divisor value of the total number of TRs in the rest scan (504 TRs). We then shifted the 36 TR window by 1 TR repeatedly until all TRs were examined. This approach demonstrated that the relationship between DMPFC social pattern reinstatement and social memory performance is significant between the initial ~1 min, 14 s to 1 min, 53 s of rest and again between ~2 min, 7 s to 2 min, 50 s. The relationship never becomes significant again later in rest (*SI Appendix*, Fig. S1). Overall, the temporal analyses add further support for the prioritization hypothesis: It is during relatively early moments of rest in which social information is preferentially consolidated by the DMPFC at rest.

In contrast to the DMPFC, the IVLPFC did not show evidence of temporal prioritization for nonsocial consolidation. There was not a greater number of nonsocial IVLPFC pattern reinstatements during early (vs. middle and late) rest periods [$t(46) = 0.90$, $P = 0.376$]. Moreover, the correlation between IVLPFC nonsocial pattern reinstatement and nonsocial memory performance was marginal during all time periods (early $\beta = 0.30$, $P = 0.145$; middle $\beta = 0.38$, $P = 0.065$; late $\beta = 0.31$, $P = 0.130$), indicating the nonsocial consolidation relationship was not unique to early rest. In other words, while IVLPFC nonsocial pattern reinstatement does preferentially relate to nonsocial memory consolidation, it does not show evidence of temporal prioritization.

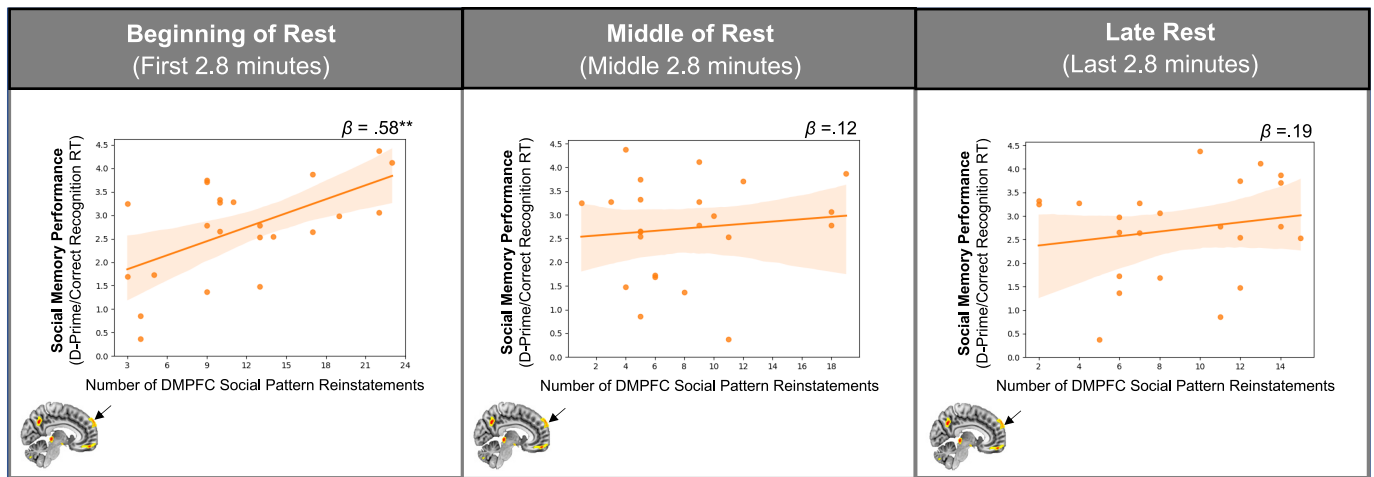


Fig. 5. The relationship between DMPFC social pattern reinstatement and subsequent social memory is driven by the early rest period.

The Hippocampus Plays a General Role in Memory Consolidation at Rest.

Given its broad role in memory consolidation (59), we next examined the hippocampus. ROIs were created from a correct vs. incorrect contrast during encoding, in which clusters emerged in both the left and right hippocampus. A multivariate template pattern for correctly remembered stimuli was extracted from encoding data within each ROI and used for pattern reinstatement analysis. Consistent with previous literature (35), we found a marginal effect indicating that the amount of correct pattern reinstatement in the right hippocampus at rest negatively predicted overall memory performance ($\beta = -0.40$, $P = 0.061$). Looking at each type of memory separately, we found a nonsignificant relationship between social correct pattern reinstatement and social memory performance ($\beta = 0.23$, $P = 0.295$), as well as nonsocial correct pattern reinstatement and nonsocial memory performance ($\beta = -0.37$, $P = 0.087$) in the right hippocampus. Additionally, the amount of correct pattern reinstatement was not greater in earlier (vs. middle and late) rest periods [$t(46) = 0.55$, $P = 0.582$].

Mean Encoding Results. Past work has demonstrated “encoding and subsequent memory” effects such that greater activation during encoding often predicts superior subsequent memory (60–62). It is therefore possible that our reinstatement results are epiphenomenal, reflecting residual effects driven by encoding. Given this possibility, we sought to explore if mean, univariate activation during encoding of social and nonsocial stimuli meaningfully predict participants’ memory scores and, if yes, to delineate the ways in which brain activity during encoding and brain activity during postencoding rest uniquely contribute to participants’ memory performance. We found, however, that neither mean, univariate activation in the DMPFC in response to social stimuli predicted social memory ($\beta = 0.11$, $P = 0.607$) nor did mean, univariate IVPFC activation in response to nonsocial stimuli predict nonsocial stimuli ($\beta = -0.32$, $P = 0.109$). We repeated this analysis examining encoding only of trials that were later accurately remembered and again found null results (DMPFC in response to social stimuli predicting social memory ($\beta = 0.11$, $P = 0.616$) nor in the IVPFC in response to nonsocial stimuli ($\beta = -0.31$, $P = 0.190$)). We hypothesize that this difference between our results and prior work could be driven by the greater complexity in the stimulus set than in previously used paradigms and the lack of a narrative structure in the stimulus set in comparison to other naturalistic stimuli designs. Overall, these follow-up analyses further point to the

important role of postencoding rest in memory consolidation, including the prioritization of social memory consolidation by the DMPFC.

Discussion

Humans are a highly social species and must learn from their social environment to succeed in everyday life (63). Yet, whether and how the brain may be tuned toward social learning and memory remains unclear. We provide evidence that the DMPFC prioritizes social learning via quick-acting consolidation processes during rest. In contrast, the IVPFC, a region previously implicated in encoding and subsequent memory effects (56, 64, 65), promotes nonsocial learning via consolidation mechanisms at rest in a non-prioritized fashion. Collectively, the findings suggest that social information may be preferentially prioritized during learning and update existing models of memory consolidation, which to date have not documented this possibility.

The findings provide key support for the suggestion that the human brain may be “social by default” (36, 37). This perspective argues that, given that the same brain regions associated with social inference comprise a great deal of the default network, a brain system characterized by activating “by default” during rest, important social cognitive processes may occur by default during rest in humans to facilitate navigating social life (36, 37). Our results support this hypothesis by showing that the DMPFC, a key default network region, helps to commit social memory traces relatively quickly during rest. Thus, the tendency to engage the DMPFC by default during rest may keep the brain in a state of readiness to facilitate social learning and memory.

Whether such default social tuning mechanisms help ensure we are socially savvy vs. the possibility that social brain mechanisms engage by default as a consequence of people tending to be very social remains to be determined. On the one hand, default network engagement at rest has been observed early in infant development (66), suggesting humans may come into the world with default network mechanisms in place to help ensure sociality. On the other hand, transitioning into contexts that amplify the need for social bonding and new social roles, such as the transition into adolescence as well as the transition to motherhood, correspond with systematic changes in default network function, including resting state patterns (67–69). Whether such changes reflect purely environmental vs. biological mechanisms remains to be fully determined. At the very least, future work could

examine how manipulating social contact impacts default social learning and memory.

The DMPFC social consolidation results are consistent with recent arguments of adaptive memory consolidation (41), which suggest that postencoding consolidation processes may prioritize goal-relevant information. This account proposes multiple dimensions that may be prioritized during consolidation, such as valence and arousal (41). Note that our social and nonsocial stimuli were matched on valence and arousal, as well as other dimensions often conflated with sociality: interestingness and familiarity. Thus, sociality may be one dimension of many that the brain “tags” for adaptive memory processes.

Systems memory consolidation is often considered a lengthy process, occurring over a night of sleep or even over several days (see ref. 30 for a review). However, extensive research suggests that the rest period directly following encoding plays a key role in the consolidation process (33, 34), even if there are times when memory systems continue to work on the information. Indeed, the observation that social information is quickly reinstated by the DMPFC is not mutually exclusive with the observation that some information continues to be processed over time. Moreover, recent work has shown that rapid offline consolidation—in the first 10 s following encoding—meaningfully predicts memory performance (70), further suggesting that early reactivation enhances consolidation.

Interestingly, the “schema assimilation model” (71) proposes that memory consolidation can be rapid if the newly encoded information aligns with preexisting schemas. Schemas refer to the abstract knowledge structures that have been developed over multiple encoding instances (72). Rodent work in support of the schema assimilation model finds that new information relevant to a preexisting schema is quickly consolidated in memory, bypasses the hippocampus, and may rely on the medial prefrontal cortex (71, 73). Prior work in humans finds the immediate postencoding connectivity between the hippocampus and MPFC also predicts the longer-term schema development in MPFC that occurs over the following week (74). This suggests processes that start during postencoding rest immediately after learning impact the long-term consolidation of schemas. On the topic of schemas, participants with preexisting, similar social schemas show similar neural responding in the DMPFC while viewing schema-relevant stimuli (49, 75). Prior work also suggests quick, spontaneous DMPFC activation accelerates social information processing (36, 37). For example, greater prestimulus DMPFC activity during very brief rest (i.e., jittered fixation) predicts faster social decisions on the next experimental trial (36, 37). Taken together, these results suggest the endogenous accessibility of social schemas (e.g., abstractions of social categories, scripts, and norms) may play a role in facilitating the quick DMPFC social pattern reinstatement results observed here. This suggestion is consistent with early theoretical accounts of perception and cognition which argue that the endogenous state we are in shapes what we perceive and think about (76). DMPFC engagement at rest may keep the brain in a prepared state, with social schemas readily accessible to facilitate social learning and memory.

Additional research will help determine the precise aspect(s) of “sociality” consolidated by the DMPFC at rest. Here, the sociality of a stimulus was determined by independent raters’ responses to the question “to what extent does this video clip have to do with people?” Experimenters subsequently confirmed all social clips had at least one human present and nonsocial clips had no humans. While the prompt provided to the independent raters is concrete, multiple features may have been considered in participants’ responses to the question. On the one hand, the DMPFC

may consolidate any information depicted of humans. Indeed, prior work shows that in human participants, the DMPFC is more active in response to scenes with humans relative to multiple other categories, including other nonhuman animals (77). On the other hand, the DMPFC may consolidate information depicting social interactions, broadly construed. One recent study showed participants videos of shapes moving on a screen. The more participants felt confident that the shapes conveyed a social interaction (e.g., a big circle “bullying” a small circle), the more they showed DMPFC activity while observing the videos (78). It is also noteworthy that the default network includes multiple brain regions in addition to the DMPFC, including the VMPFC, precuneus, temporoparietal junction, and superior temporal sulcus extending into temporal poles. It is thus possible that while the DMPFC prioritizes certain social information during consolidation, additional default network regions may prioritize other types of content and/or processes relevant to social life.

More broadly, findings from the current study contribute to a greater understanding of default network function. One current account of default network function proposes that the default network may process higher-order, internally constructed representations (79, 80). Alternatively, to integrate findings that implicate the default network in social cognition, others have more recently proposed the default network may integrate extrinsic social information (e.g., witnessing someone make a social blunder) and intrinsic information idiosyncratic to their internal experience (e.g., remembering how you felt the last time you made a social blunder) to create shared social knowledge across individuals (e.g., “we all agree that the person we saw should feel embarrassed”; 81). Results from our study propose one possible mechanism by which the default network may integrate extrinsic social information and intrinsic, idiosyncratic information: via social cognitive consolidation functions at rest.

We also observed pattern reinstatement in the hippocampus, as well as IPPA, negatively correlated with overall memory performance (collapsing across social and nonsocial stimuli) in a non-prioritized fashion. The hippocampus finding supports the prior work our reinstatement approach was based on, which also found that hippocampal pattern reinstatement helps commit weakly learned information to memory (35). Specifically, Schapiro et al. (35) instructed participants to learn three sets of novel shapes and found greater hippocampal reinstatement predicted better memory for the weakly learned shapes (i.e., a negative correlation between reinstatement and memory performance). Similarly, research in rodents examining hippocampal replay finds that the relationship between encoding and replay is not always positively correlated and that hippocampal replay may serve to build representations of the entire environment, rather than just the well-learned aspects (82). Given that the PPA is structurally close to the hippocampus, and that our nonsocial items were less well-remembered than the social items, this region may operate similarly to the hippocampus—prioritizing memory consolidation for weakly learned places.

One surprising result was that there were more DMPFC nonsocial (vs. social) pattern reinstatements. That said, the number of nonsocial DMPFC reinstatements did not predict subsequent nonsocial memory, suggesting despite being frequently reinstated, this reinstatement is not functionally relevant for nonsocial memory consolidation. Although speculative, we suspect these results reflect the fact that social and nonsocial stimuli were observed in the same encoding session and were taken from the same documentary, *Samsara*. The documentary includes footage of people from 25 different countries, as well as scenic footage from those same 25 countries. As a result, the social clips (e.g., footage of

people praying) are related to nonsocial clips (e.g., footage of a temple). It is possible that while observing the nonsocial scenes, participants call to mind (through the DMPFC) related social clips and/or try to tie the nonsocial and social scenes together during encoding. Importantly though, the nonsocial memory test directs participants' attention toward recognizing the scene (rather than its link to social clips). During the recognition test, participants may therefore focus on the perceptual, nonsocial features of the test item, something dealt with by the IVLPFC nonsocial pattern reinstatements. This would explain why the number of DMPFC nonsocial patterns during rest is high and does not predict subsequent nonsocial memory. Consistent with this possibility, prior work has found that when nonsocial stimuli are perceived as reflecting social information, the DMPFC engages (78). More work is needed to understand whether and how the DMPFC may imbue social meaning onto nonsocial stimuli during memory consolidation.

Limitations. There are two noteworthy limitations to our study. First, the sample size is relatively small. The number of participants recruited was based on the sample size used in the prior work the reinstatement approach was based on (35). Future research on social memory consolidation in larger samples will be useful. Second, reinstatement was defined as the number of times the correlation between the encoding pattern and TR rest pattern is 1.5 SDs above the mean for a given subject. We used this approach to align with previous research (35), facilitating direct comparisons with prior findings. That said, there are likely other ways to define reinstatement—for example with the strength of correlation between encoding and rest TRs. Additional methods development may be needed to further assess the multifaceted nature of memory consolidation during rest.

Conclusion. In summary, we found that when left with the choice to consolidate social or nonsocial information, the human brain prioritizes consolidating social information during rest first. This process happens through the DMPFC, a key node of the brain's default network—which gets its name from the observation that it activates by default whenever our mind is free from external demands. Our results therefore suggest that the tendency to default to the DMPFC may help ensure we learn new social information as soon as we can.

Methods

Participants. Twenty-six individuals (17 females; 9 males; mean age = 22.77, SD = 4.8; 65.38% White, 23.08% Asian or Pacific Islander, 7.69% Black, 3.85% Other; 3.85% Hispanic) were recruited for participation in the study. The full study protocol was approved by the Dartmouth College Institutional Review Board. All participants provided informed consent. Participants were awarded course credit or paid \$20 per hour for study completion.

Stimuli. Stimuli presented at encoding consisted of 5 to 10 s video clip excerpts from the non-narrative, documentary film, *Samsara*. A total of 60 video clips were presented at encoding, 30 of which were social stimuli (e.g., showed footage of humans) and 30 of which were nonsocial stimuli (e.g., showed footage of locations and industrial objects).

A total of 120 stimuli were selected based on ratings from mTurk participants ($n = 372$) who previewed 389 video clips from *Samsara*. Participants were presented with 65 video clips and rated each clip they saw on dimensions of familiarity, valence, pleasantness, excitement, and sociality. Ratings were made on a scale from 1 to 100 (where 1 = low familiarity, low pleasantness, low excitement, or negative valence and 100 = high familiarity, high pleasantness, high excitement, or positive valence). Mean ratings of familiarity, valence, pleasantness, and excitement were not statistically significantly different across social and nonsocial

video clips (t 's < 0.59, P 's > 0.53), but mean ratings of sociality did significantly differ (Mean social videos = 71.60, SD = 9.43; Mean nonsocial videos = 34.63; SD = 6.58; $t = -28.97$; $P = 1.40e-36$).

As noted elsewhere in the paper, we chose stimuli from the documentary, *Samsara*, because it was intentionally developed to have no narrative, helping ensure observed results have more to do with sociality than narrative perception. As an additional assurance, we collected another sample of MTurk participants ($N = 60$), who rated the selected social and nonsocial video clips. This sample rated each video along two dimensions: 1) the extent to which they had to do with people (i.e., sociality as in the original sample of raters) and 2) the extent to which they conveyed a narrative. Analyses on these ratings support the idea that the sociality of the video clips, rather than narrative perception, discriminates the stimuli. First, the difference between sociality ratings for the social vs. nonsocial stimuli was larger than the difference between the narrative ratings [$F(1, 59) = 372.41$, $P < 0.001$]. In fact, inspecting the mean ratings of each variable showed that participants perceived that the social videos had more to do with people ($M = 62.44$, $SD = 14.85$) than narratives [$M = 19.26$, $SD = 20.40$, $t(59) = 15.63$, $P < 0.001$], whereas the nonsocial videos were perceived to convey narratives ($M = 6.34$, $SD = 8.08$) more so than be about people [$M = 2.24$, $SD = 4.76$, $t(59) = 4.27$, $P < 0.001$]. Second, the social videos are perceived as significantly more social than the nonsocial videos when controlling for the extent to which they conveyed a narrative [$F(1, 58) = 656.10$, $P < 0.001$]. Third, the difference in sociality ratings for the two stimulus types (social vs. nonsocial) did not significantly interact with their narrative ratings [$F(1, 58) = 1.09$, $P = 0.302$]. This third result indicates that the differences of socialness in the stimulus types do not covary with their difference in narrative perception.

Procedures. Participants completed an fMRI scanning session consisting of a structural anatomical scan, two encoding scans, a postencoding rest scan, and subsequently, a surprise memory test.

Encoding. To mimic the way we simultaneously encounter social and nonsocial information in everyday life, at encoding, social and nonsocial video clips were randomly presented, as opposed to being blocked. Jittered fixation occurred after each video clip [mean interstimulus interval (ISI) = 3.00 s; SD = 0.825 s]. Each participant completed two encoding functional runs lasting 11 min.

Resting State. Next, participants completed a resting state scan. At rest, participants were instructed to think about what they wanted and stay awake. Based on prior research examining consolidation during rest, each rest scan lasted 8.4 min (39, 83).

Memory Test. After the postencoding resting state scan, participants completed a surprise memory test where they indicated if the image on the screen was shown to them at encoding by selecting "Yes," "No," or "I don't know." Participants had up to 6 s to respond and were presented with 120 images of 60 social and 60 nonsocial stimuli. The test was made up of 60 true images shown at encoding, and 60 lure images taken from video clips of documentary film, *Samsara*, but not shown during the encoding phase. Stimulus images were randomly presented across participants. Our memory performance variable takes into account both accuracy and speed. Specifically, we calculated the d' memory score by subtracting standardized false alarms from standardized hits with z -scores derived via the inverse cumulative density function. This value was then divided by the speed (i.e., RT) with which it took participants to answer accurately (i.e., $d'/\text{correct RT}$). The $d'/\text{correct RT}$ scores were linked to neural reinstatement because 1) they take both accuracy and speed into account and 2) they demonstrated more variability across participants than d' alone. As an additional step to assess the robustness of our memory results, we examined whether there were systematic differences in hit and false alarm rates between social and nonsocial stimuli, as well as whether our reinstatement-to-subsequent memory results replicate when hits are considered the outcome variable. These results are reported in *SI Appendix*, though briefly, the results indicate that our memory findings are not simply due to differences in stimulus discriminability and the brain-behavior findings persist when hits are examined.

fMRI Data Acquisition. Brain imaging was conducted at the Dartmouth Brain Imaging Center in Hanover, NH on a Siemens Prisma 3T scanner using a 32-channel head coil. Functional images were acquired with a T2*-weighted echo-planar imaging sequence set to the following parameters: voxel size = 2.5 x 2.5 x 2.5 mm, repetition time (TR) = 1,000 ms, echo time (TE) = 30 ms, field of

view (FoV) = 24 cm, slice thickness = 2.5-mm, matrix = 96 x 96, flip angle = 59°, multiband acceleration factor = 4. Each participant also underwent a T1-weighted structural image (voxel size = 0.9-mm, TR = 2,300 ms, TE = 2.32 ms, FoV = 24 cm, slice thickness = 0.9-mm, matrix = 256 x 256, and flip angle = 8°). The study design consisted of an event-related randomized design determined by easy-optimize-x (84) to maximize detection of meaningful neural clusters from the linear contrasts of interest at encoding (i.e., social vs. nonsocial encoding), which later serve as ROIs for reinstatement analyses.

fMRI Data Preprocessing. Results included in this manuscript come from preprocessing performed using fMRIPrep 20.2.2 (85); RRID:SCR_016216), which is based on Nipype 1.6.1 (86); RRID:SCR_002502). As recommended by the creators of fMRIPrep, the preprocessing steps are reported below verbatim from the software output.

Anatomical Data Preprocessing. A total of 1 T1-weighted (T1w) images were found within the input BIDS dataset. The T1-weighted (T1w) image was corrected for intensity nonuniformity (INU) with N4BiasFieldCorrection (87), distributed with ANTs 2.3.3 (88); RRID:SCR_004757, and used as T1w-reference throughout the workflow. The T1w-reference was then skull-stripped with a Nipype implementation of the antsBrainExtraction.sh workflow (from ANTs), using OASIS30ANTs as target template. Brain tissue segmentation of cerebrospinal fluid (CSF), white matter (WM) and gray matter (GM) was performed on the brain-extracted T1w using fast [FSL 5.0.9; RRID:SCR_002823, (89)]. Volume-based spatial normalization to one standard space (MNI152NLin2009cAsym) was performed through nonlinear registration with antsRegistration (ANTs 2.3.3), using brain-extracted versions of both T1w reference and the T1w template. The following template was selected for spatial normalization: ICBM 152 Nonlinear Asymmetrical template version 2009c [(90); RRID:SCR_008796; TemplateFlow ID: MNI152NLin2009cAsym].

Functional Data Preprocessing. For each of the BOLD runs found per subject (across all tasks and sessions), the following preprocessing was performed. First, a reference volume and its skull-stripped version were generated using a custom methodology of fMRIPrep. Head-motion parameters with respect to the BOLD reference (transformation matrices, and six corresponding rotation and translation parameters) are estimated before any spatiotemporal filtering using mcflirt [FSL 5.0.9, (91)]. Susceptibility distortion correction (SDC) was omitted. The BOLD time series (including slice-timing correction when applied) were resampled onto their original, native space by applying the transforms to correct for head-motion. These resampled BOLD time series will be referred to as preprocessed BOLD in original space, or just preprocessed BOLD. The BOLD reference was then coregistered to the T1w reference using flirt [FSL 5.0.9, (92)] with the boundary-based registration (93) cost function. Coregistration was configured with nine degrees of freedom to account for distortions remaining in the BOLD reference. Several confounding time series were calculated based on the preprocessed BOLD: framewise displacement (FD), DVARS, and three region-wise global signals. FD was computed using two formulations following Power [absolute sum of relative motions, (94)] and Jenkinson [relative rms displacement between affines, (91)]. FD and DVARS are calculated for each functional run, both using their implementations in Nipype [following the definitions by Power et al. (94)]. The three global signals are extracted within the CSF, the WM, and the whole-brain masks. Additionally, a set of physiological regressors were extracted to allow for component-based noise correction [CompCor, (95)]. Principal components are estimated after high-pass filtering the preprocessed BOLD time series (using a discrete cosine filter with 128 s cutoff) for the two CompCor variants: temporal (tCompCor) and anatomical (aCompCor). tCompCor components are then calculated from the top 2% variable voxels within the brain mask. For aCompCor, three probabilistic masks (CSF, WM, and combined CSF+WM) are generated in anatomical space. The implementation differs from that of Behzadi et al. in that instead of eroding the masks by 2 pixels on BOLD space, the aCompCor masks are subtracted a mask of pixels that likely contain a volume fraction of GM. This mask is obtained by thresholding the corresponding partial volume map at 0.05, and it ensures components are not extracted from voxels containing a minimal fraction of GM. Finally, these masks are resampled into BOLD space and binarized by thresholding at 0.99 (as in the original implementation). Components are also calculated separately within the WM and CSF masks. For each CompCor decomposition, the *k* components with the largest singular values are retained, such that the retained components' time series are sufficient to explain 50 percent of variance across the nuisance mask

(CSF, WM, combined, or temporal). The remaining components are dropped from consideration. The head-motion estimates calculated in the correction step were also placed within the corresponding confounds file. The confound time series derived from head motion estimates and global signals were expanded with the inclusion of temporal derivatives and quadratic terms for each (96). Frames that exceeded a threshold of 0.5 mm FD or 1.5 standardized DVARS were annotated as motion outliers. The BOLD time series were resampled into standard space, generating a preprocessed BOLD run in MNI152NLin2009cAsym space. First, a reference volume and its skull-stripped version were generated using a custom methodology of fMRIPrep. All resamplings can be performed with a single interpolation step by composing all the pertinent transformations (i.e., head-motion transform matrices, SDC when available, and coregistrations to anatomical and output spaces). Gridded (volumetric) resamplings were performed using antsApplyTransforms (ANTs), configured with Lanczos interpolation to minimize the smoothing effects of other kernels (97). Nongridded (surface) resamplings were performed using mri_vol2surf (FreeSurfer).

General Linear Model. Neuroimaging data were analyzed using NLTools (98). The data were spatially smoothed using a 6-mm full-width half-maximum 3D Gaussian kernel. Nuisance variables included in the model consisted of 6 head motion parameters (*x*, *y*, and *z* directions of roll, pitch, and yaw rotations), a high-pass filter (duration 128 s), linear and quadratic filters, and run regressors. TRs in non-steady-state and TRs with spikes in global signal and average frame difference greater than 3 SDs were included as individual regressors.

For functional data obtained during encoding scans, a general linear model was created for each participant to estimate task-induced activation during social and nonsocial stimulus presentation. Stimulus presentation regressors were convolved with a Glover hemodynamic response function. For functional data obtained during resting state scans, an additional intercept regressor was included to remove global signal (94). All resting state analyses were performed on the remaining residual time series.

First-level, univariate contrasts comparing social and nonsocial stimuli at encoding were generated for each subject from the model-estimated data. Second-level analyses were subsequently performed to derive ROIs. These group contrasts were statistically thresholded at $P < 0.001$ with a cluster extent of 200 voxels. The social vs. nonsocial contrast revealed significant clusters of activity in the DMPFC ($x = 12$ $y = 52$ $z = 40$, $k = 501$), VMPFC ($x = 4$ $y = 52$ $z = -18$, $k = 517$), precuneus ($x = 6$ $y = -60$ $z = 34$, $k = 313$), left amygdala ($x = -20$ $y = -8$ $z = -14$, $k = 16,433$), and left fusiform gyrus ($x = -44$ $y = -50$ $z = -20$, $k = 4,572$). The nonsocial vs. social contrast revealed significant clusters of activity in bilateral parahippocampal place area ($x = -34$ $y = -48$ $z = -2$, $k = 1,243$; $x = 32$ $y = -40$ $z = -4$, $k = 1,149$) and left VLPFC ($x = -34$ $y = 48$ $z = 26$, $k = 262$).

An additional first-level, univariate contrast comparing activity during encoding of trials that were later correctly vs. incorrectly remembered was generated for each subject. Second-level analyses were statistically thresholded at $P < 0.001$ with a cluster extent of 30 voxels, given the relatively small anatomical size of the hippocampus and to help ensure we had a hippocampal cluster to investigate. The correct vs. incorrect contrast revealed significant clusters of activity in the bilateral hippocampus ($x = -20$ $y = -8$ $z = -16$, $k = 36$; $x = 20$ $y = -6$ $z = -18$, $k = 38$) and right parahippocampal gyrus ($x = 32$ $y = -76$ $z = -22$, $k = 1,504$).

We also ran first-level analyses to derive mean univariate activity during social encoding (vs. implicit baseline) and separately, nonsocial encoding (vs. implicit baseline). This allowed us to perform "encoding-and-subsequent memory" analyses. Specifically, we assessed whether univariate activity in the DMPFC during social encoding predicted subsequent social memory performance, as well as whether univariate activity in the VLPFC during nonsocial encoding predicted subsequent nonsocial memory performance. We also performed a first-level analysis to assess whether mean univariate activity during social and nonsocial encoding for stimuli that were later correctly remembered related to subsequent memory performance. These were follow-up analyses to assess the extent to which effects observed in these two regions during postencoding rest were influenced by the overall level of activity in these regions during encoding.

Follow-up whole-brain analyses were performed using the $k = 50$ whole-brain parcellation that used *k*-means clustering to isolate meta-analytic coactivations from Neurosynth (99). This parcellation was chosen to help ensure that the regions selected are functionally relevant to psychological constructs.

Whole-brain reinstatement analyses were multiple comparisons corrected using a Bonferroni-corrected P -value of 0.001.

Pattern Reinstatement. Multivariate template patterns were created using beta values extracted from functional ROIs identified in first-level contrasts at encoding. The multivariate template patterns from encoding were correlated with the multivariate template pattern within the same functional ROI for each TR during postencoding rest (TRs = 504), generating a matrix of correlation values for each template pattern across the duration of rest. Consistent with the research our approach is based on (35), a potential reinstatement was defined as a correlation greater than 1.5 SD above the mean of all correlations for a given subject. The amount of correlation values that exceeded this threshold were summed across postencoding rest to generate a count metric used in subsequent analyses. Consistent with prior social consolidation work (39), memory performance scores and reinstatement values from the full rest periods were excluded if greater than 2 SDs away from the group mean. This corresponded with one social memory outlier, two social DMPFC outliers, one nonsocial DMPFC outlier, two social IVPFC outliers, one nonsocial IVPFC outlier, and two hippocampus outliers removed from their respective variables. Brain-behavior correlations reported in the manuscript reflect two-tailed P -values.

This study was explicitly designed to assess condition-level reinstatement. Thus, multivariate template patterns derived at encoding and used in subsequent reinstatement analysis are generated from social encoding (vs. implicit baseline,

i.e., mean activation of all social stimuli at encoding) and nonsocial encoding (vs. implicit baseline; i.e., mean activation of all nonsocial stimuli at encoding) as opposed to individual stimuli. These condition-level representations are then correlated with each TR of postencoding rest to assess reinstatement related to subsequent memory performance. That said, we ran exploratory item-level reinstatement models to further probe our DMPFC findings (See *SI Appendix* for more details).

As a follow-up, we ran control analyses in which we generated an encoding template for which the beta values were randomly sampled from the social and nonsocial encoding templates. Thus, this template consisted of a mix of partial social and nonsocial representations at encoding randomly spatially distributed throughout the template. Further, we ran another control analysis in which the encoding template was simply the average of both the social and nonsocial encoding templates, thus representing all stimuli at encoding.

Data, Materials, and Software Availability. Anonymized behavioral and ROI data have been deposited in the Open Science Framework: <https://osf.io/dmf7k/> (100).

ACKNOWLEDGMENTS. This research was supported by an R01 awarded to Dr. Meghan L. Meyer. Portions of this work were developed from the master's thesis of Courtney Jimenez.

1. S. J. Luck, E. K. Vogel, The capacity of visual working memory for features and conjunctions. *Nature* **390**, 279–281 (1997).
2. G. A. Alvarez, P. Cavanagh, The capacity of visual short-term memory is set both by visual information load and by number of objects. *Psychol. Sci.* **15**, 106–111 (2004).
3. M. A. Cohen, T. L. Botch, C. E. Robertson, The limits of color awareness during active, real-world vision. *Proc. Natl. Acad. Sci. U.S.A.* **117**, 13821–13827 (2020).
4. D. L. Schacter, The seven sins of memory. Insights from psychology and cognitive neuroscience. *Am. Psychol.* **54**, 182–203 (1999).
5. C. E. Looser, J. S. Guntupalli, T. Wheatley, Multivoxel patterns in face-sensitive temporal regions reveal an encoding schema based on detecting life in a face. *Soc. Cogn. Affect. Neurosci.* **8**, 799–805 (2013).
6. S. T. Fiske, S. E. Taylor, *Social Cognition: From Brains to Culture* (SAGE, 2013).
7. J. P. Mitchell, Social psychology as a natural kind. *Trends Cogn. Sci.* **13**, 246–251 (2009).
8. J. Bowlby, *A Secure Base: Parent-Child Attachment and Healthy Human Development* (Routledge, 1988).
9. H. F. Harlow, The nature of love. *Am. Psychol.* **13**, 673–685 (1958).
10. R. L. Repetti, S. E. Taylor, T. E. Seeman, Risky families: Family social environments and the mental and physical health of offspring. *Psychol. Bull.* **128**, 330–366 (2002).
11. J. B. Silk, S. C. Alberts, J. Altmann, Social bonds of female baboons enhance infant survival. *Science* **302**, 1231–1234 (2003).
12. R. O. Deaner, A. V. Khera, M. L. Platt, Monkeys pay per view: Adaptive valuation of social images by rhesus macaques. *Curr. Biol.* **15**, 543–548 (2005).
13. J. S. Nairne, S. R. Thompson, J. N. S. Pandeirada, Adaptive memory: Survival processing enhances retention. *J. Exp. Psychol. Learn. Mem. Cogn.* **33**, 263–273 (2007).
14. V. P. Murty, R. Alison Adcock, *The Hippocampus from Cells to Systems* (Springer International Publishing, 2017).
15. E. A. Mientlarzewska, D. Bavelier, S. Schwartz, Influence of reward motivation on human declarative memory. *Neurosci. Biobehav. Rev.* **61**, 156–176 (2016).
16. D. L. Hamilton, L. B. Katz, V. O. Leirer, Cognitive representation of personality impressions: Organizational processes in first impression formation. *J. Pers. Soc. Psychol.* **39**, 1050–1063 (1980).
17. D. M. Werchan, D. Amso, All contexts are not created equal: Social stimuli win the competition for organizing reinforcement learning in 9-month-old infants. *Dev. Sci.* **24**, e13088 (2021).
18. J. P. Mitchell, C. N. Macrae, M. R. Banaji, Encoding-specific effects of social cognition on the neural correlates of subsequent memory. *J. Neurosci.* **24**, 4912–4917 (2004).
19. Z. Chen, K. D. Williams, J. Fitness, N. C. Newton, When hurt will not heal: Exploring the capacity to relieve social and physical pain. *Psychol. Sci.* **19**, 789–795 (2008).
20. M. D. Lieberman, M. A. Straccia, M. L. Meyer, M. Du, K. M. Tan, Social, self, (situational), and affective processes in medial prefrontal cortex (MPFC): Causal, multivariate, and reverse inference evidence. *Neurosci. Biobehav. Rev.* **99**, 311–328 (2019).
21. A. K. Martin, I. Dzafic, S. Ramdave, M. Meinzer, Causal evidence for task-specific involvement of the dorsomedial prefrontal cortex in human social cognition. *Soc. Cogn. Affect. Neurosci.* **12**, 1209–1218 (2017).
22. D. D. Wagner, W. M. Kelley, J. V. Haxby, T. F. Heatherton, The dorsal medial prefrontal cortex responds preferentially to social interactions during natural viewing. *J. Neurosci.* **36**, 6917–6925 (2016).
23. R. Báez-Mendoza, E. P. Mastroianni, A. J. Wang, Z. M. Williams, Social agent identity cells in the prefrontal cortex of interacting groups of primates. *Science* **374**, eabb4149 (2021).
24. G. L. Shulman *et al.*, Common blood flow changes across visual tasks: II. Decreases in cerebral cortex. *J. Cogn. Neurosci.* **9**, 648–663 (1997).
25. M. E. Raichle *et al.*, A default mode of brain function. *Proc. Natl. Acad. Sci. U.S.A.* **98**, 676–682 (2001).
26. M. E. Raichle, The brain's default mode network. *Annu. Rev. Neurosci.* **38**, 433–447 (2015).
27. M. F. Carr, S. P. Jadhav, L. M. Frank, Hippocampal replay in the awake state: A potential substrate for memory consolidation and retrieval. *Nat. Neurosci.* **14**, 147–153 (2011).
28. M. P. Karlsson, L. M. Frank, Awake replay of remote experiences in the hippocampus. *Nat. Neurosci.* **12**, 913–918 (2009).
29. A. Tambini, N. Ketz, L. Davachi, Enhanced brain correlations during rest are related to memory for recent experiences. *Neuron* **65**, 280–290 (2010).
30. Y. Dudai, The restless engram: Consolidations never end. *Annu. Rev. Neurosci.* **35**, 227–247 (2012).
31. R. Stickgold, Sleep-dependent memory consolidation. *Nature* **437**, 1272–1278 (2005).
32. M. P. Walker, R. Stickgold, Sleep-dependent learning and memory consolidation. *Neuron* **44**, 121–133 (2004).
33. A. Tambini, L. Davachi, Awake reactivation of prior experiences consolidates memories and biases cognition. *Trends Cogn. Sci.* **23**, 876–890 (2019).
34. A. Tambini, M. D'Esposito, Causal contribution of awake post-encoding processes to episodic memory consolidation. *Curr. Biol.* **30**, 3533–3543.e7 (2020).
35. A. C. Schapiro, E. A. McDevitt, T. T. Rogers, S. C. Mednick, K. A. Norman, Human hippocampal replay during rest prioritizes weakly learned information and predicts memory performance. *Nat. Commun.* **9**, 3920 (2018).
36. R. P. Spunt, M. L. Meyer, M. D. Lieberman, The default mode of human brain function primes the intentional stance. *J. Cogn. Neurosci.* **27**, 1116–1124 (2015).
37. M. L. Meyer, Social by default: Characterizing the social functions of the resting brain. *Curr. Dir. Psychol. Sci.* **28**, 380–386 (2019).
38. A. B. Satpute, D. Badre, K. N. Ochsner, Distinct regions of prefrontal cortex are associated with the controlled retrieval and selection of social information. *Cereb. Cortex* **24**, 1269–1277 (2014).
39. M. L. Meyer, L. Davachi, K. N. Ochsner, M. D. Lieberman, Evidence that default network connectivity during rest consolidates social information. *Cereb. Cortex* **29**, 1910–1920 (2019).
40. E. Collier, M. L. Meyer, Memory of others' disclosures is consolidated during rest and associated with providing support: Neural and linguistic evidence. *J. Cogn. Neurosci.* **32**, 1672–1687 (2020).
41. E. T. Cowan, A. C. Schapiro, J. E. Dunsmoor, V. P. Murty, Memory consolidation as an adaptive process. *Psychon. Bull. Rev.* **28**, 1796–1810 (2021).
42. R. F. Baumeister, M. R. Leary, The need to belong: Desire for interpersonal attachments as a fundamental human motivation. *Psychol. Bull.* **117**, 497–529 (1995).
43. E. A. Kensinger, S. Corkin, Memory enhancement for emotional words: Are emotional words more vividly remembered than neutral words? *Mem. Cognit.* **31**, 1169–1180 (2003).
44. S. McGillivray, K. Murayama, A. D. Castel, Thirst for knowledge: The effects of curiosity and interest on memory in younger and older adults. *Psychol. Aging* **30**, 835–841 (2015).
45. A. P. Yonelinas, The nature of recollection and familiarity: A review of 30 years of research. *J. Mem. Lang.* **46**, 441–517 (2002).
46. S. A. Nastase *et al.*, The "Narratives" fMRI dataset for evaluating models of naturalistic language comprehension. *Sci. Data* **8**, 250 (2021).
47. C. Baldassano, U. Hasson, K. A. Norman, Representation of real-world event schemas during narrative perception. *J. Neurosci.* **38**, 9689–9699 (2018).
48. J. Chen *et al.*, Accessing real-life episodic information from minutes versus hours earlier modulates hippocampal and high-order cortical dynamics. *Cereb. Cortex* **26**, 3428–3441 (2016).
49. E. S. Finn, P. R. Corlett, G. Chen, P. A. Bandettini, R. T. Constable, Trait paranoia shapes inter-subject synchrony in brain activity during an ambiguous social narrative. *Nat. Commun.* **9**, 2043 (2018).
50. E. Redday, D. Moraczewski, Social cognition in context: A naturalistic imaging approach. *Neuroimage* **216**, 116392 (2020).
51. E. Simony *et al.*, Dynamic reconfiguration of the default mode network during narrative comprehension. *Nat. Commun.* **7**, 12141 (2016).
52. A. K. Lee, M. A. Wilson, Memory of sequential experience in the hippocampus during slow wave sleep. *Neuron* **36**, 1183–1194 (2002).
53. T. J. Davidson, F. Kloosterman, M. A. Wilson, Hippocampal replay of extended experience. *Neuron* **63**, 497–507 (2009).
54. K. Diba, G. Buzsáki, Forward and reverse hippocampal place-cell sequences during ripples. *Nat. Neurosci.* **10**, 1241–1242 (2007).
55. D. J. Foster, M. A. Wilson, Reverse replay of behavioural sequences in hippocampal place cells during the awake state. *Nature* **440**, 680–683 (2006).
56. D. Badre, A. D. Wagner, Left ventrolateral prefrontal cortex and the cognitive control of memory. *Neuropsychologia* **45**, 2883–2901 (2007).

57. L. Nadel, M. Moscovitch, Memory consolidation, retrograde amnesia and the hippocampal complex. *Curr. Opin. Neurobiol.* **7**, 217–227 (1997).
58. T. Yarkoni, R. A. Poldrack, T. E. Nichols, D. C. Van Essen, T. D. Wager, Large-scale automated synthesis of human functional neuroimaging data. *Nat. Methods* **8**, 665–670 (2011).
59. H. Eichenbaum, T. Otto, N. J. Cohen, The hippocampus—What does it do? *Behav. Neural Biol.* **57**, 2–36 (1992).
60. P. C. Fletcher, C. M. E. Stephenson, T. A. Carpenter, T. Donovan, E. T. Bullmore, Regional brain activations predicting subsequent memory success: An event-related fMRI study of the influence of encoding tasks. *Cortex* **39**, 1009–1026 (2003).
61. H. Kim, Neural activity that predicts subsequent memory and forgetting: A meta-analysis of 74 fMRI studies. *Neuroimage* **54**, 2446–2461 (2011).
62. M. R. Uncapher, A. D. Wagner, Posterior parietal cortex and episodic encoding: Insights from fMRI subsequent memory effects and dual-attention theory. *Neurobiol. Learn. Mem.* **91**, 139–154 (2009).
63. R. I. M. Dunbar, The social brain hypothesis and its implications for social evolution. *Ann. Hum. Biol.* **36**, 562–572 (2009).
64. I. Kahn *et al.*, Transient disruption of ventrolateral prefrontal cortex during verbal encoding affects subsequent memory performance. *J. Neurophysiol.* **94**, 688–698 (2005).
65. H. Park, M. D. Rugg, Neural correlates of successful encoding of semantically and phonologically mediated inter-item associations. *Neuroimage* **43**, 165–172 (2008).
66. W. Gao *et al.*, Evidence on the emergence of the brain's default network from 2-week-old to 2-year-old healthy pediatric subjects. *Proc. Natl. Acad. Sci. U.S.A.* **106**, 6790–6795 (2009).
67. F. Fan *et al.*, Development of the default-mode network during childhood and adolescence: A longitudinal resting-state fMRI study. *Neuroimage* **226**, 117581 (2021).
68. E. Hoekzema *et al.*, Pregnancy leads to long-lasting changes in human brain structure. *Nat. Neurosci.* **20**, 287–296 (2017).
69. L. H. Somerville *et al.*, The medial prefrontal cortex and the emergence of self-conscious emotion in adolescence. *Psychol. Sci.* **24**, 1554–1562 (2013).
70. M. Bönstrup *et al.*, A rapid form of offline consolidation in skill learning. *Curr. Biol.* **29**, 1346–1351.e4 (2019).
71. D. Tse *et al.*, Schemas and memory consolidation. *Science* **316**, 76–82 (2007).
72. V. E. Ghosh, A. Gilboa, What is a memory schema? A historical perspective on current neuroscience literature. *Neuropsychologia* **53**, 104–114 (2014).
73. D. Tse *et al.*, Schema-dependent gene activation and memory encoding in neocortex. *Science* **333**, 891–895 (2011).
74. A. Tomparny, L. Davachi, Consolidation promotes the emergence of representational overlap in the hippocampus and medial prefrontal cortex. *Neuron* **96**, 228–241.e5 (2017).
75. Y. C. Leong, J. Chen, R. Willer, J. Zaki, Conservative and liberal attitudes drive polarized neural responses to political content. *Proc. Natl. Acad. Sci. U.S.A.* **117**, 27731–27739 (2020).
76. J. S. Bruner, On perceptual readiness. *Psychol. Rev.* **64**, 123–152 (1957).
77. D. D. Wagner, W. M. Kelley, T. F. Heatherton, Individual differences in the spontaneous recruitment of brain regions supporting mental state understanding when viewing natural social scenes. *Cereb. Cortex* **21**, 2788–2796 (2011).
78. R. S. Varrier, E. S. Finn, Seeing social: A neural signature for conscious perception of social interactions. *J. Neurosci.* **42**, 9211–9226 (2022).
79. R. L. Buckner, L. M. DiNicola, The brain's default network: Updated anatomy, physiology and evolving insights. *Nat. Rev. Neurosci.* **20**, 593–608 (2019).
80. J. Smallwood *et al.*, The default mode network in cognition: A topographical perspective. *Nat. Rev. Neurosci.* **22**, 503–513 (2021).
81. Y. Yeshurun, M. Nguyen, U. Hasson, The default mode network: Where the idiosyncratic self meets the shared social world. *Nat. Rev. Neurosci.* **22**, 181–192 (2021).
82. A. S. Gupta, M. A. A. van der Meer, D. S. Touretzky, A. D. Redish, Hippocampal replay is not a simple function of experience. *Neuron* **65**, 695–705 (2010).
83. A. Tambini, U. Rimmele, E. A. Phelps, L. Davachi, Emotional brain states carry over and enhance future memory formation. *Nat. Neurosci.* **20**, 271–278 (2017).
84. B. Spunt, Easy-optimize-x: Formal Release for Archiving on Zenodo (1.0). Zenodo. <https://doi.org/10.5281/zenodo.58616>. Deposited 25 July 2016.
85. O. Esteban *et al.*, fMRIPrep: a robust preprocessing pipeline for functional MRI. *Nat. Methods* **16**, 111–116 (2019).
86. K. Gorgolewski, *et al.*, Nipype: a flexible, lightweight and extensible neuroimaging data processing framework in python. *Front. Neuroinform.* **5**, 13 (2011).
87. N. J. Tustison *et al.*, N4ITK: Improved N3 bias correction. *IEEE Trans. Med. Imaging* **29**, 1310–1320 (2010).
88. B. B. Avants, C. L. Epstein, M. Grossman, J. C. Gee, Symmetric diffeomorphic image registration with cross-correlation: Evaluating automated labeling of elderly and neurodegenerative brain. *Med. Image Anal.* **12**, 26–41 (2008).
89. Y. Zhang, M. Brady, S. Smith, Segmentation of brain MR images through a hidden Markov random field model and the expectation-maximization algorithm. *IEEE Trans. Med. Imaging* **20**, 45–57 (2001).
90. V. Fonov *et al.*, Unbiased average age-appropriate atlases for pediatric studies. *Neuroimage* **54**, 313–327 (2011).
91. M. Jenkinson, P. Bannister, M. Brady, S. Smith, Improved optimization for the robust and accurate linear registration and motion correction of brain images. *Neuroimage* **17**, 825–841 (2002).
92. M. Jenkinson, S. Smith, A global optimisation method for robust affine registration of brain images. *Med. Image Anal.* **5**, 143–156 (2001).
93. D. N. Greve, B. Fischl, Accurate and robust brain image alignment using boundary-based registration. *Neuroimage* **48**, 63–72 (2009).
94. J. D. Power *et al.*, Methods to detect, characterize, and remove motion artifact in resting state fMRI. *Neuroimage* **84**, 320–341 (2014).
95. Y. Behzadi, K. Restom, J. Liu, T. T. Liu, A component based noise correction method (CompCor) for BOLD and perfusion based fMRI. *Neuroimage* **37**, 90–101 (2007).
96. T. D. Satterthwaite *et al.*, An improved framework for confound regression and filtering for control of motion artifact in the preprocessing of resting-state functional connectivity data. *Neuroimage* **64**, 240–256 (2013).
97. C. Lanczos, Evaluation of noisy data. *J. Soc. Ind. Appl. Math. B Numer. Anal.* **1**, 76–85 (1964).
98. L. Chang, E. Jolly, J. H. Cheong, A. Burnashev, A. Chen, covanlab/nltools: 0.3.11 (Zenodo, Genève). <https://doi.org/10.5281/zenodo.2229813>.
99. A. de la Vega, L. J. Chang, M. T. Banich, T. D. Wager, T. Yarkoni, Large-scale meta-analysis of human medial frontal cortex reveals tripartite functional organization. *J. Neurosci.* **36**, 6553–6562 (2016).
100. C. A. Jimenez, M. L. Meyer, Data from “Samsara Social Consolidation.” Open Science Framework. <https://osf.io/dmf7k/>. Deposited 29 May 2023.